Supporting Information

Comparing Molybdenum and Rhenium Oxo Bis-Pyrazine-Dithiolene Complexes – In Search of an Alternative Metal Center for Molybdenum Cofactor Models

Nicolas Chrysochos,[a] Mohsen Ahmadi,[a] Stefan Malte Wahlefeld,[b] Yvonne Rippers,[b] Ingo Zebger,[b] Maria Andrea Mroginski,[b] Carola Schulzke*,[a]

[a]*Institut für Biochemie, Universität Greifswald, Felix-Hausdorff-Straße 4, 17487 Greifswald, Germany*

[b]*Institut für Chemie, Physikalische Chemie/Biophysikalische Chemie, Technische Universität Berlin, Germany*

*E-Mail: carola.schulzke@uni-greifswald.de

Table S1: Redox potentials ($E_{1/2}^0$) vs. Fc/Fc^+ for the redox transition $M^{IV} \leftrightarrow M^{V}$ for IIa $[MoO(pdt)_2]^{2-}$ and IIb $[ReO(pdt)_2]^-$ at various temperatures between 278.15 K and 338.15 K.

T [K]	IIa $[MoO(pdt)_2]^{2-}$ [V]			IIb $[ReO(pdt)_2]^{-}$ [V]		
278.15	-0.5	-0.51	-0.52	-2.07	-2.06	-1.92
283.15	-0.52	-0.51	-0.52	-2.07	-2.06	-2.06
288.15	-0.48	-0.5	-0.51	-2.07	-2.08	-1.94
293.15	-0.52	-0.5	-0.51	-2.08	-2.09	-2.11
298.15	-0.48	-0.45	-0.45	-2.24	-1.98	-1.94
298.15	-0.52	-0.5	-0.51	-2.09	-2.08	-2.06
303.15	-0.52	-0.49	-0.5	-2.09	-2.11	-2.14
308.15	-0.48	-0.45	-0.46	-2.24	-2.02	-1.96
313.15	-0.51	-0.49	-0.51	-2.1	-2.12	-2.15
318.15	-0.48	-0.47	-0.47	-2.24	-2.07	-1.96
323.15	-0.5	-0.49	-0.5	-2.1	-2.13	-2.15
328.15	-0.48	-0.46	-0.47	-2.2	-2.09	-2.01
333.15	-0.5	-0.48	-0.49	-2.12	-2.12	-2.15
338.15	-0.49	-0.46	-0.48	-2.15	-2.11	-2.09

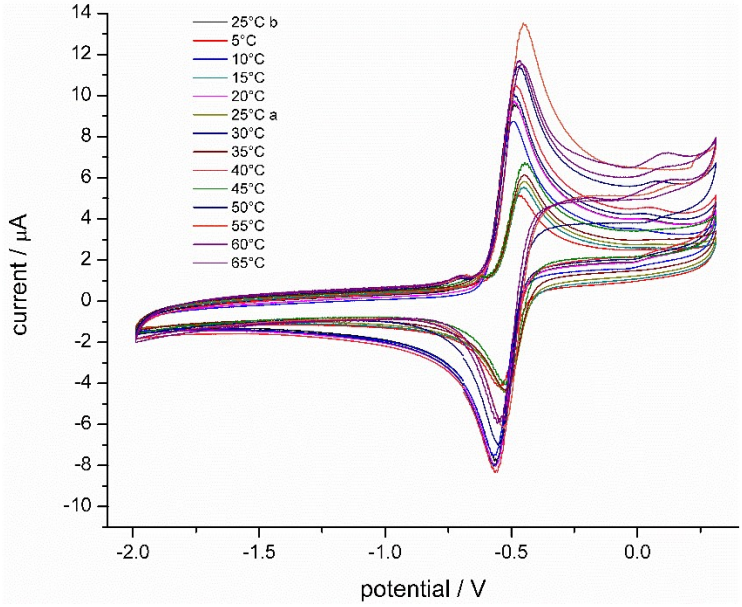

Figure S1. First measurement cyclic voltammograms of $(Et_4N)_2$[IIa] at varius temperatures between 5˚C and 65˚C in CH_3CN (0.1 mol/l Bu_4NPF). Data is referenced against Fc/Fc^+ (= 0 V in this diagram).

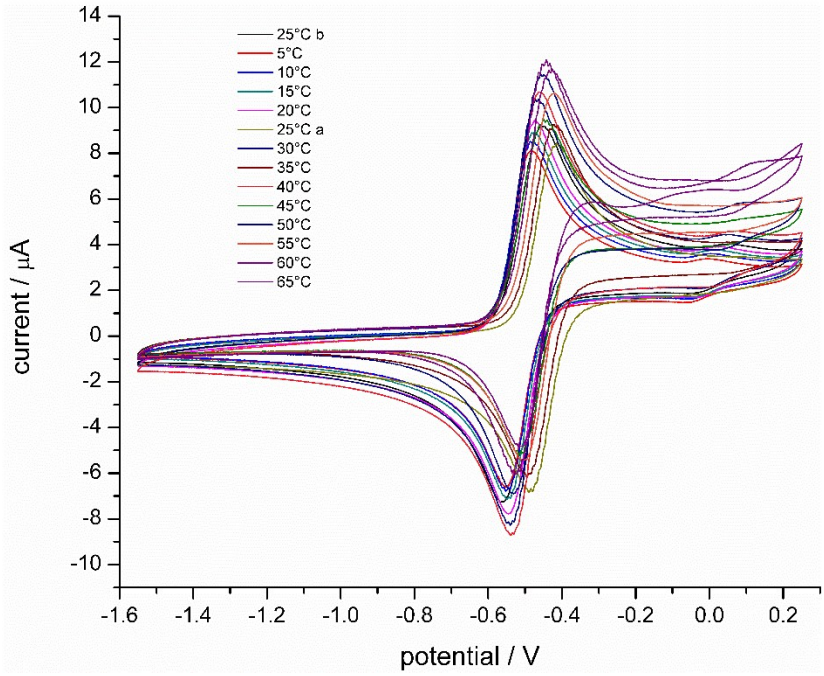

Figure S2. Second measurement cyclic voltammograms of $(Et_4N])_2$[IIa] at varius temperatures between 5˚C and 65˚C in CH_3CN (0.1 mol/l Bu_4NPF). Data is referenced against Fc/Fc^+ (= 0 V in this diagram).

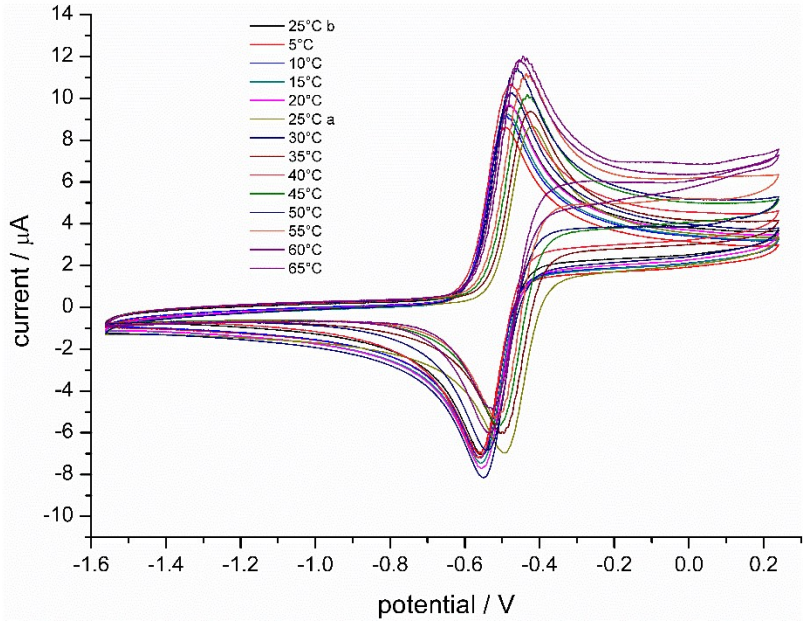

Figure S3. Third measurement cyclic voltammograms of $(Et_4N)_2$[IIa] at varius temperatures between 5˚C and 65˚C in CH_3CN (0.1 mol/l Bu_4NPF). Data is referenced against Fc/Fc^+ (= 0 V in this diagram).

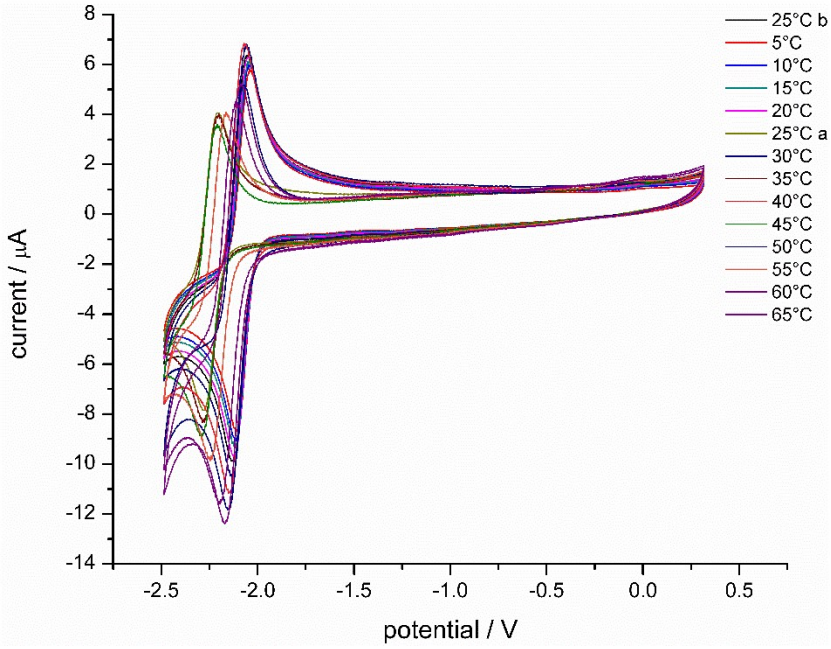

Figure S4. First measurement cyclic voltammograms of K[IIb] at varius temperatures between 5˚C and 65˚C in CH_3CN (0.1 mol/l Bu_4NPF). Data is referenced against Fc/Fc^+ (= 0 V in this diagram).

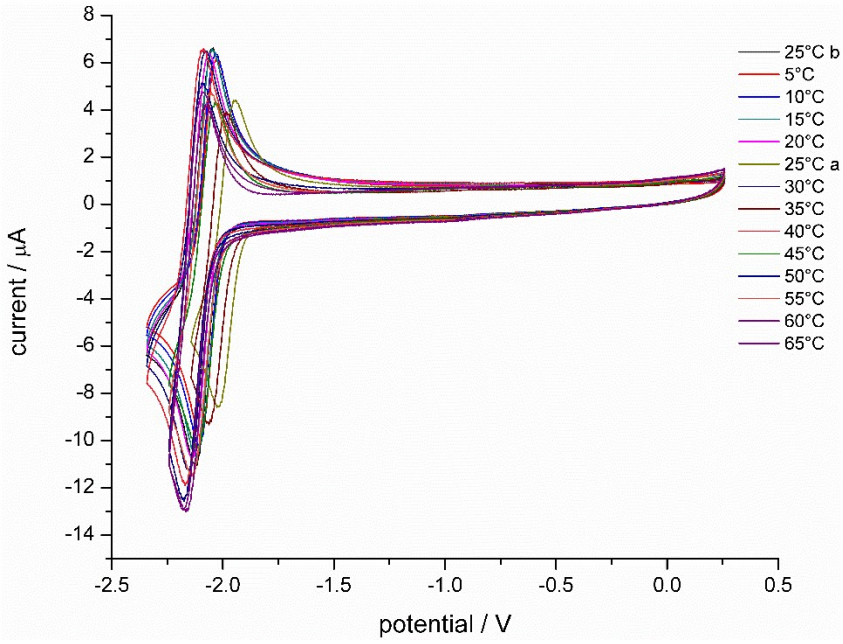

Figure S5. Second measurement cyclic voltammograms of K[IIb] at varius temperatures between 5˚C and 65˚C in CH_3CN (0.1 mol/l Bu_4NPF). Data is referenced against Fc/Fc^+ (= 0 V in this diagram).

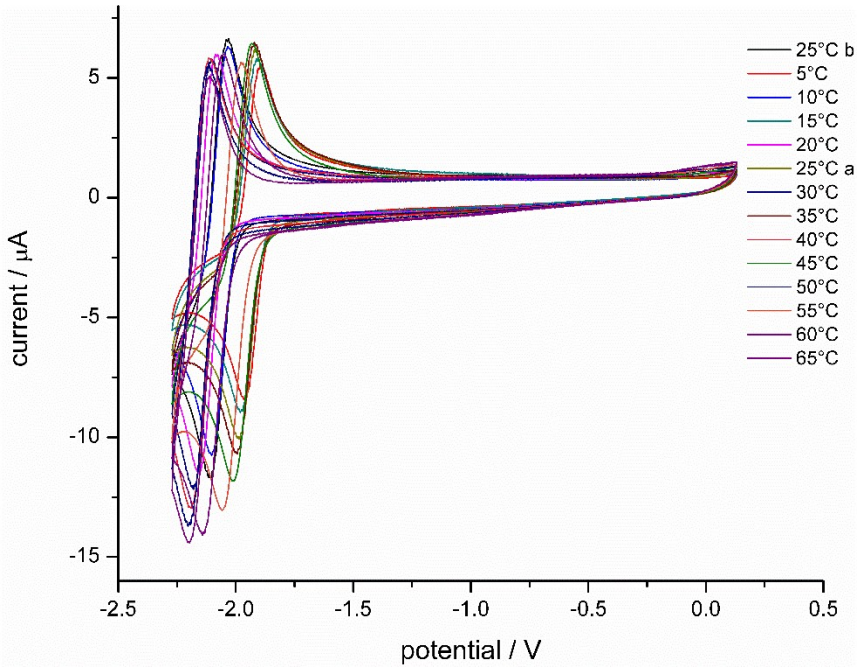

Figure S6. Third measurement cyclic voltammograms of K[IIb] at varius temperatures between 5˚C and 65˚C in CH_3CN (0.1 mol/l Bu_4NPF). Data is referenced against Fc/Fc^+ (= 0 V in this diagram).

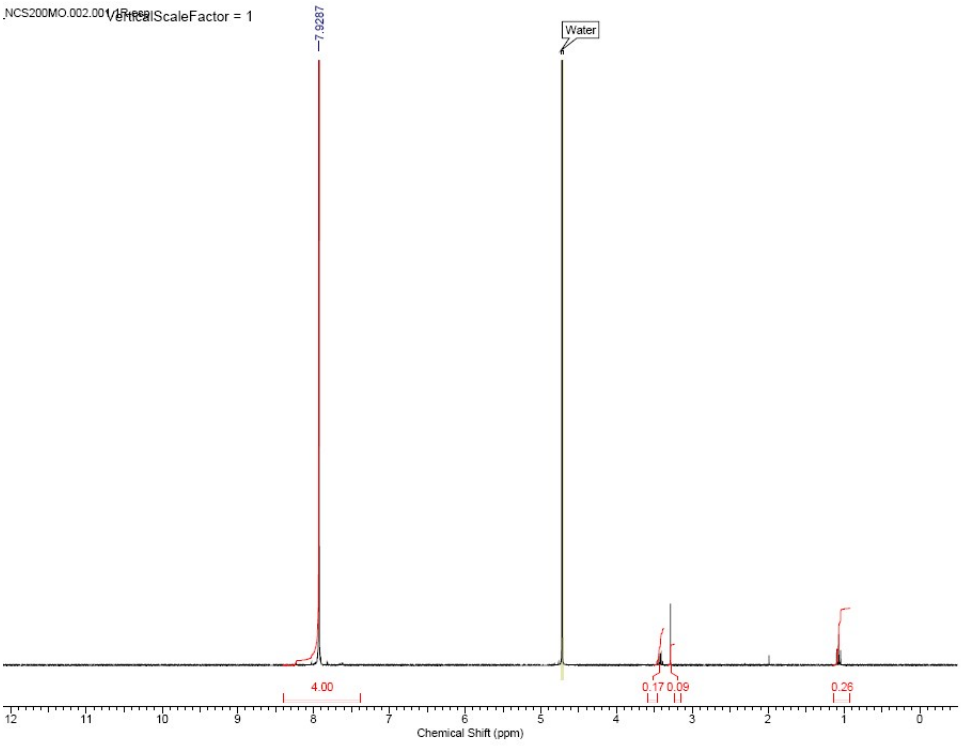

Figure S7. The 300 MHz ^1H NMR spectrum of compound K_2[IIa] in D_2O.

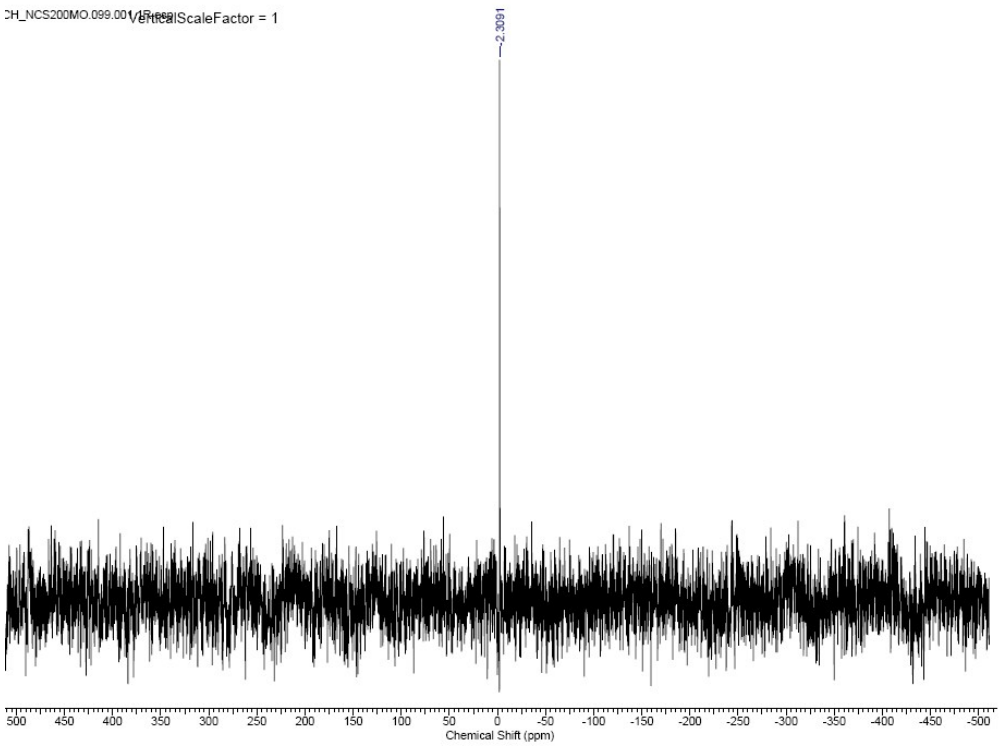

Figure S8. The 19.56 MHz ^{95}Mo-NMR spectrum of compound K_2[IIa] in D_2O.

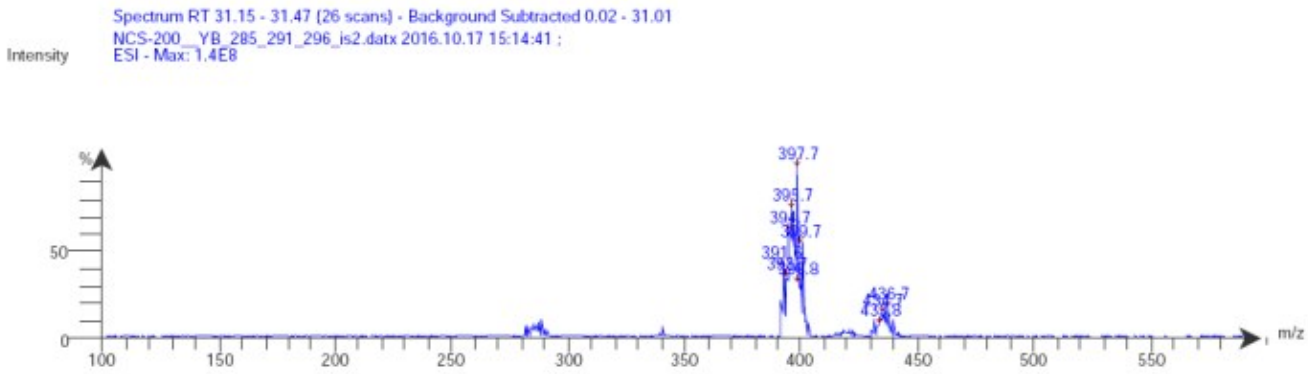

Figure S9. ESI MS spectrum from dissolution of $K_2[MoO(pdt)_2]$ (K_2[IIa]) in methanol showing its adduct $[C_8H_4N_4OMoS_4]^{2-}$ at 397.8 m/e and $[C_8H_4N_4OMoS_4]^{2-}K^+$ at 436.7 m/e.

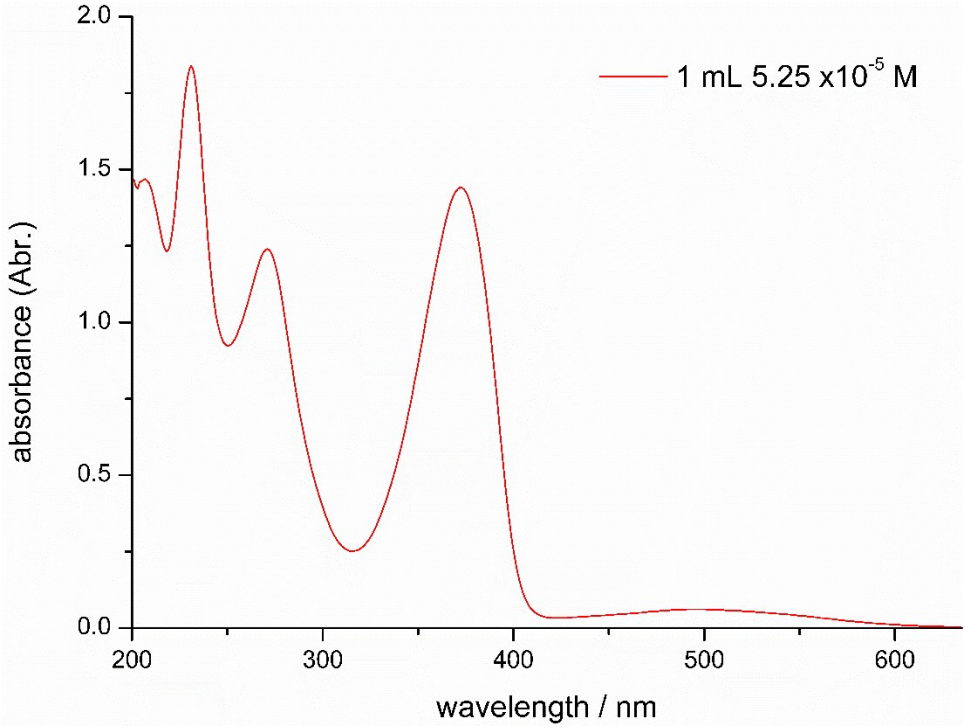

Figure S10. UV-Vis spectrum of compound $K_2[MoO(pdt)_2]$ (K_2[IIa]) in methanol at 25˚C.

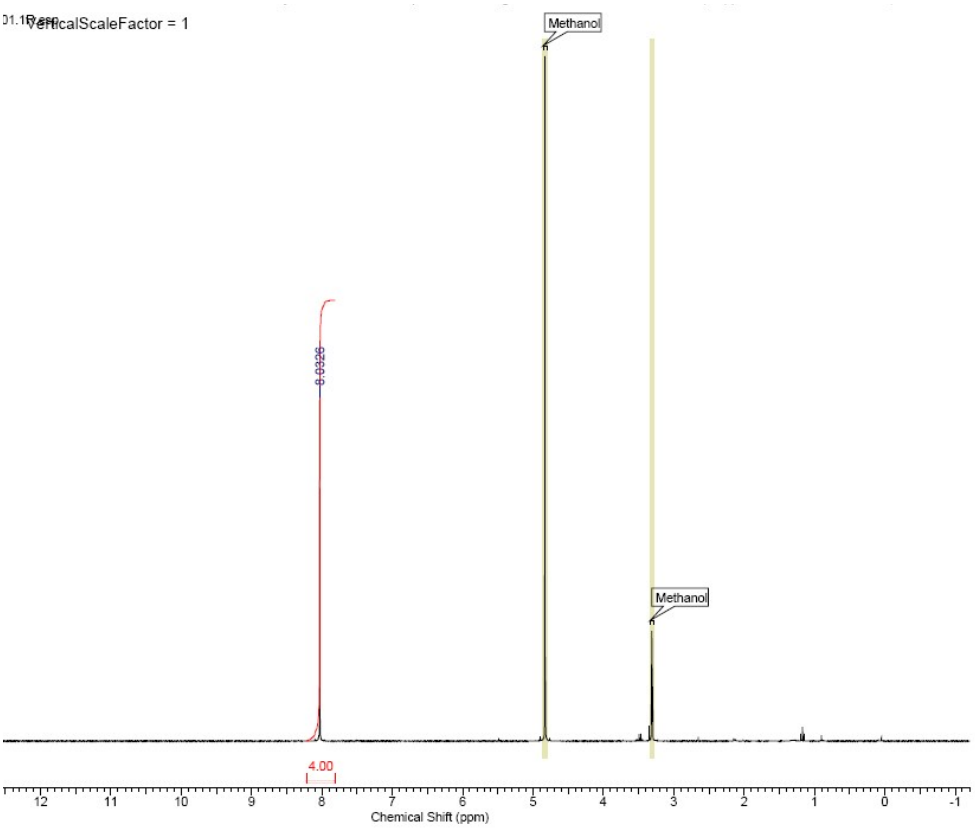

Figure S11. The 300 MHz ^{1}H NMR spectrum of compound K[IIb] in CD_3OD.

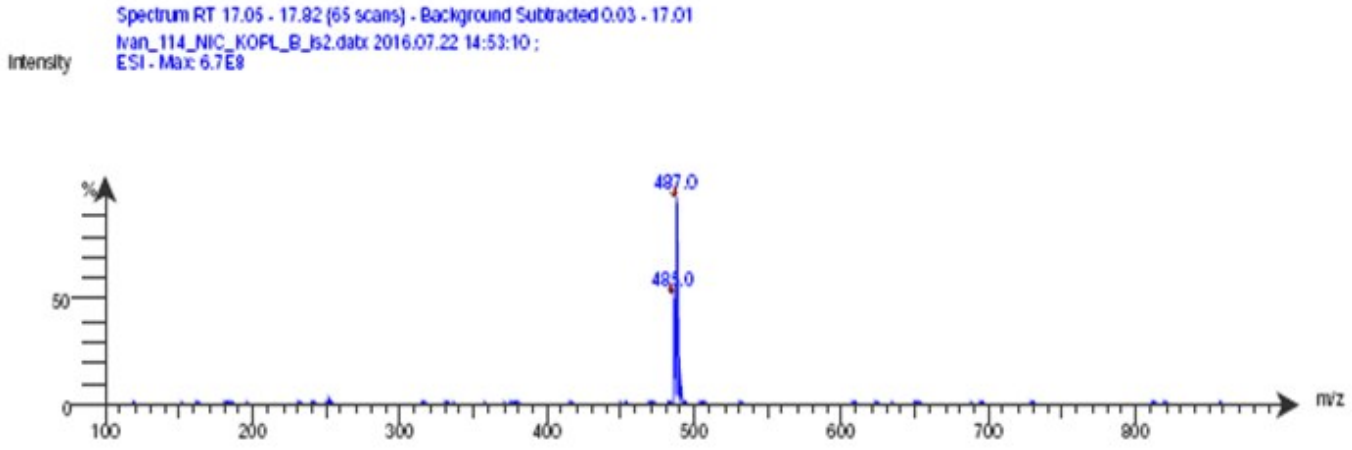

Figure S12. ESI MS spectrum from dissolution of K[ReO(pdt)$_2$] (K[IIb]) in methanol showing its adduct $[C_8H_4N_4OReS_4]^-$ at 486.6 m/e.

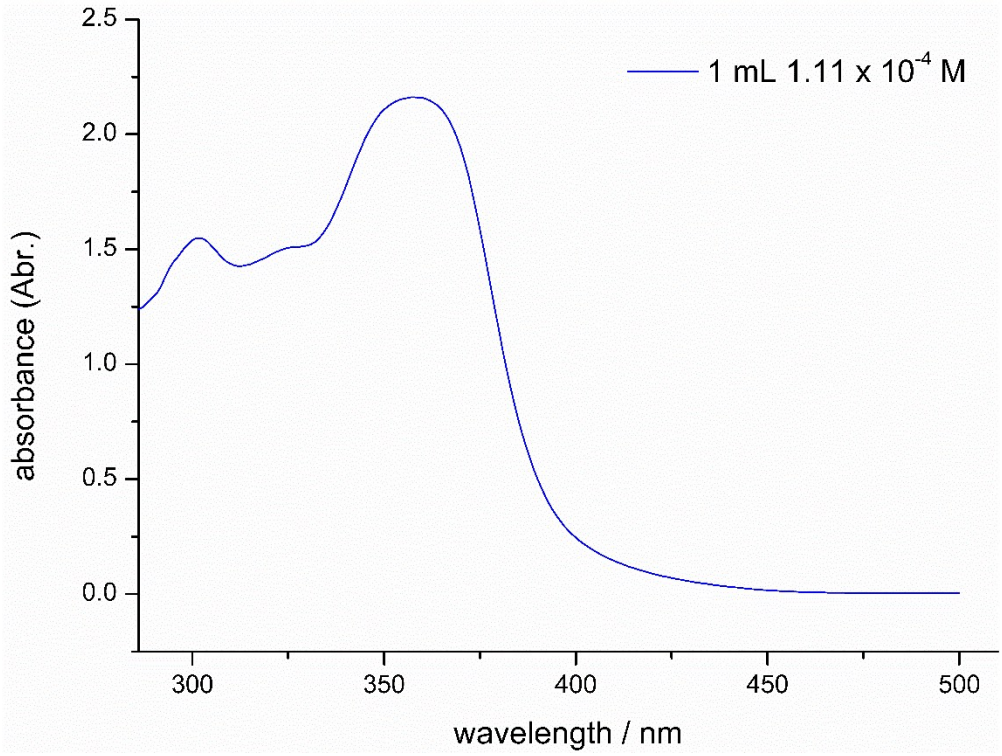

Figure S13. UV-Vis spectrum of compound K[ReO(pdt)$_2$] (K[IIb]) in methanol at 25˚C.

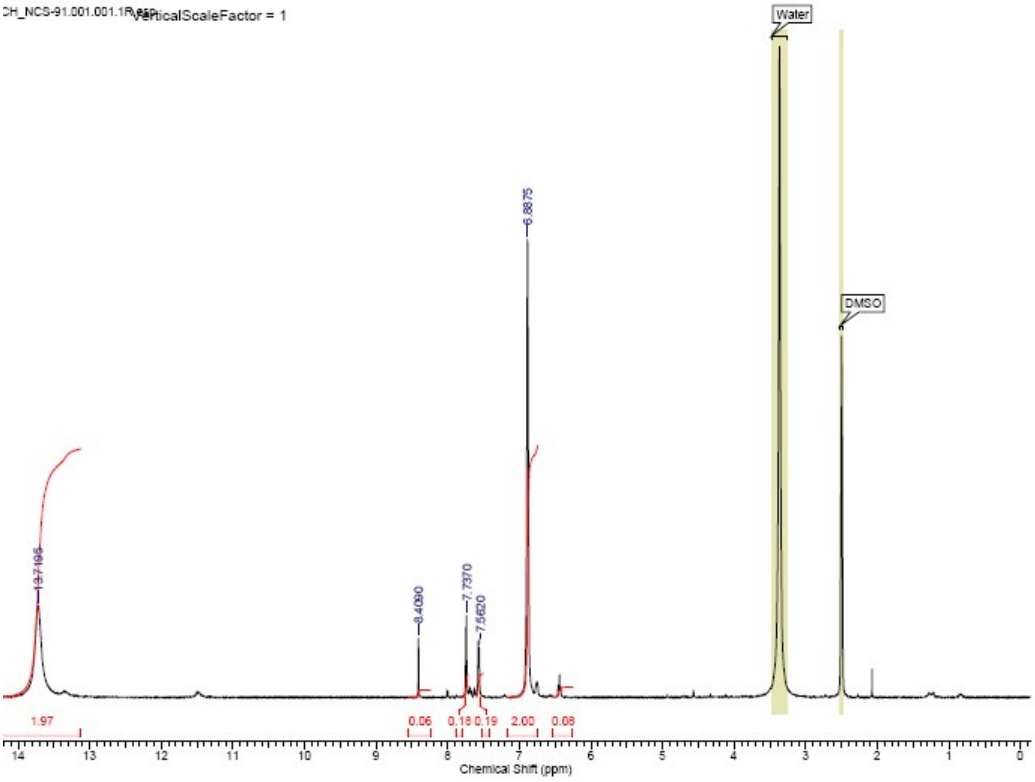

Figure S14. The 300 MHz ^{1}H NMR spectrum of compound I in DMSO-D6.

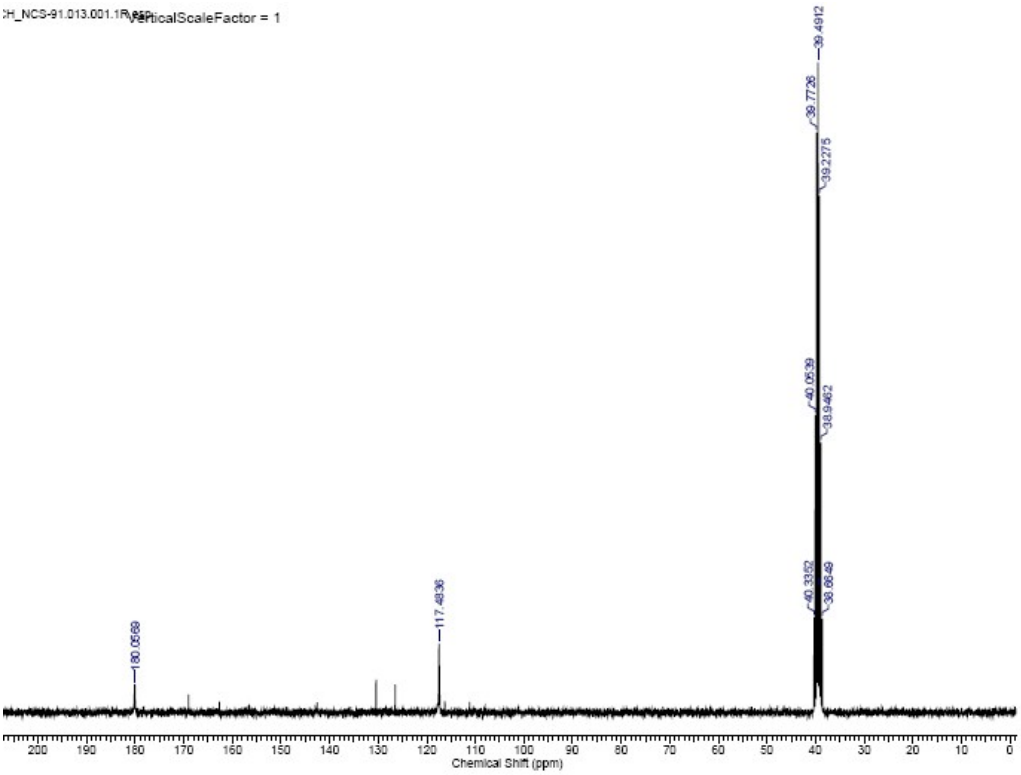

Figure S15. The 75.5 MHz ^{13}C NMR spectrum of compound I in DMSO-D6.

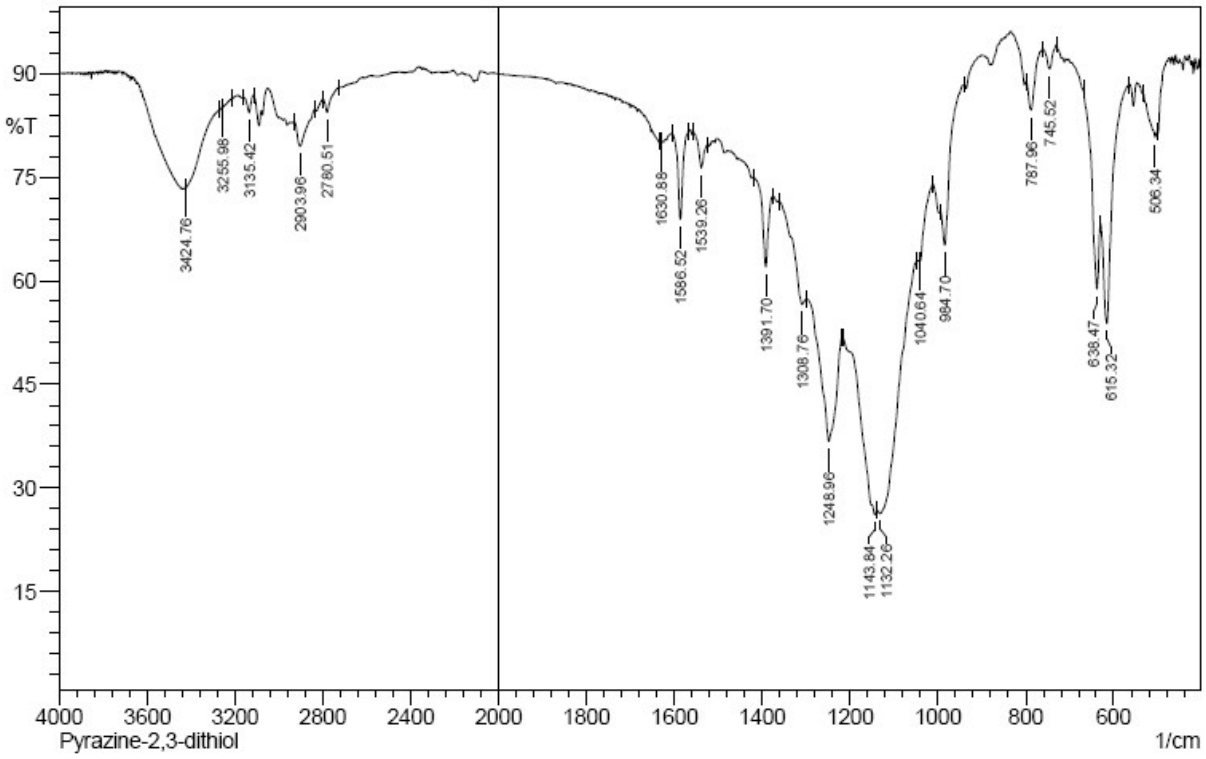

Figure S16. The IR spectrum of compound I.

Table S2 Metrical hydrogen bond parameters in $(Et_4N)_2$[IIa]. In red: hydrogen bonds involving the terminal oxido ligand (Mo=O).

D-H...A	d(D-H) / Å	d(H...A) / Å	d(D...A) / Å	<(DHA) / °
C(4)-H(4)...S(1)#1	0.95	3.00	3.755(4)	1380
C(4)-H(4)...S(3)#1	0.95	2.75	3.633(4)	1544
C(8)-H(8)...S(2)#2	0.95	2.91	3.614(4)	1323
C(8)-H(8)...S(4)#2	0.95	2.83	3.543(4)	1321
C(9)-H(9A)...S(2)#3	0.99	3.02	3.959(5)	1596
C(10)-H(10A)...O(1)	0.98	2.62	3.404(6)	1374
C(11)-H(11A)...S(4)#3	0.99	2.87	3.855(4)	1742
C(12)-H(12C)...S(2)#2	0.98	3.00	3.729(5)	1319
C(13)-H(13A)...N(2)#2	0.99	2.53	3.463(5)	1580
C(14)-H(14B)...O(2)#4	0.98	2.48	3.433(6)	1651
C(15)-H(15B)...S(4)	0.99	3.01	3.930(5)	1543
C(17)-H(17B)...O(1)#5	0.99	2.60	3.510(5)	1527
C(19)-H(19B)...S(2)	0.99	2.97	3.915(5)	1608
C(20)-H(20B)...N(4)#6	0.98	2.67	3.409(7)	1321
C(21)-H(21B)...O(1)#5	0.99	2.57	3.498(5)	1560
C(23)-H(23A)...N(2)	0.99	2.67	3.646(6)	1690
O(2)-H(1O2)...N(3)#1	0.88(6)	2.29(6)	3.152(6)	167(6)
O(2)-H(2O2)...N(1)	0.88(6)	2.10(6)	2.968(5)	171(8)

Symmetry transformations used to generate equivalent atoms: #1 -x,y+1/2,-z+1, #2 -x+1,y-1/2,-z+2, #3 x+1,y,z, #4 x+1,y,z+1, #5 -x+1,y+1/2,-z+1, #6 -x+1,y+1/2,-z+2

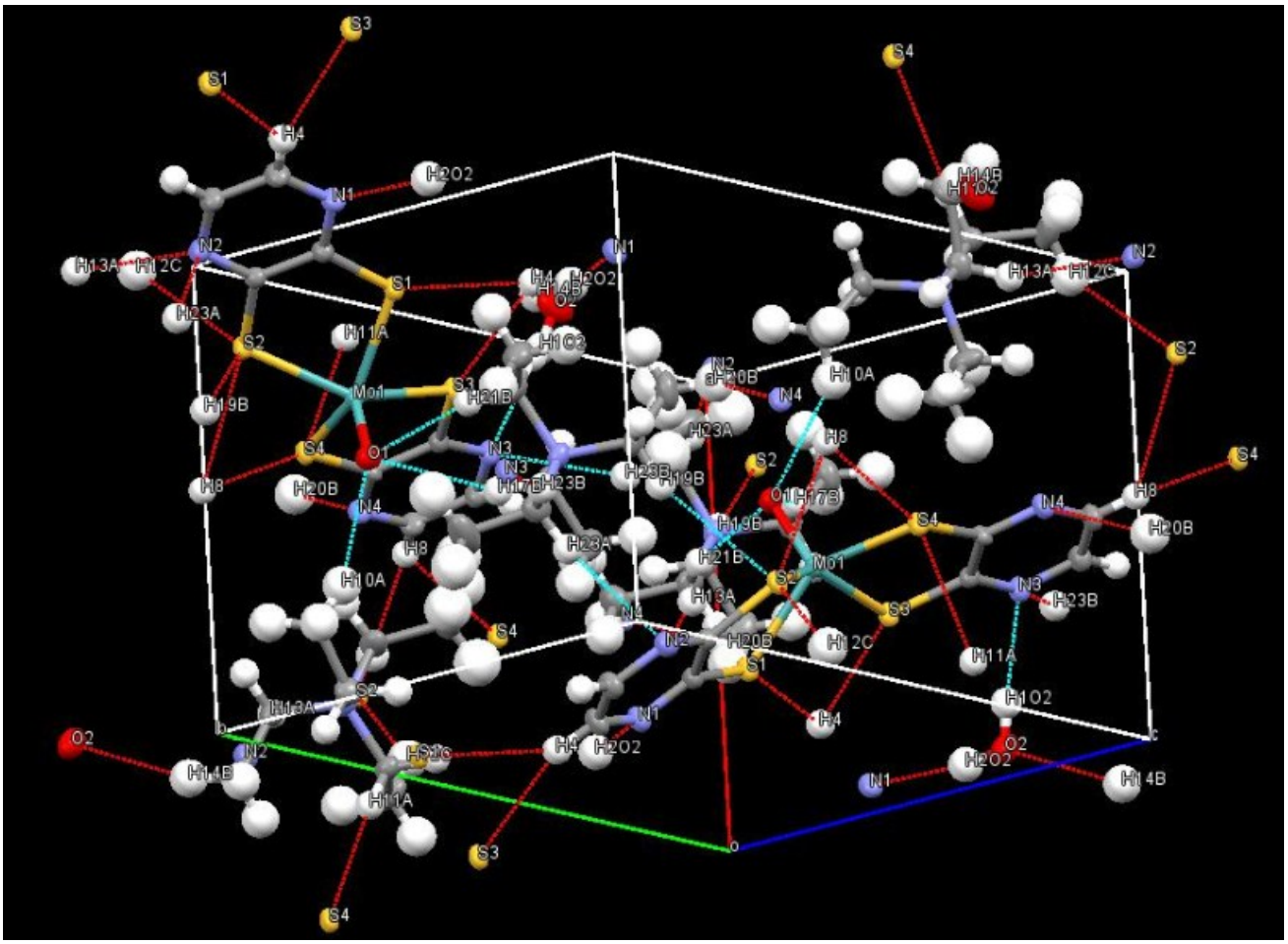

Figure S17. Uni-cell packing of compound $(Et_4N)_2$[IIa] with hydrogen bonds shown as dashed lines.

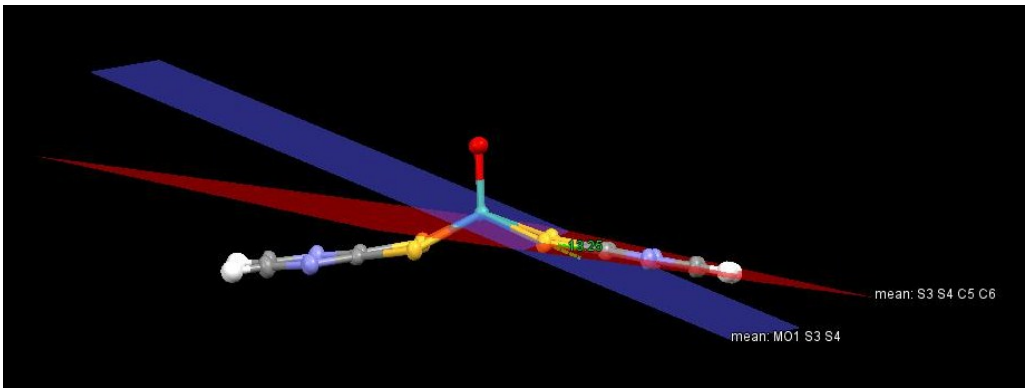

Figure S18. Fold angle a of compound $(Et_4N)_2$[IIa].

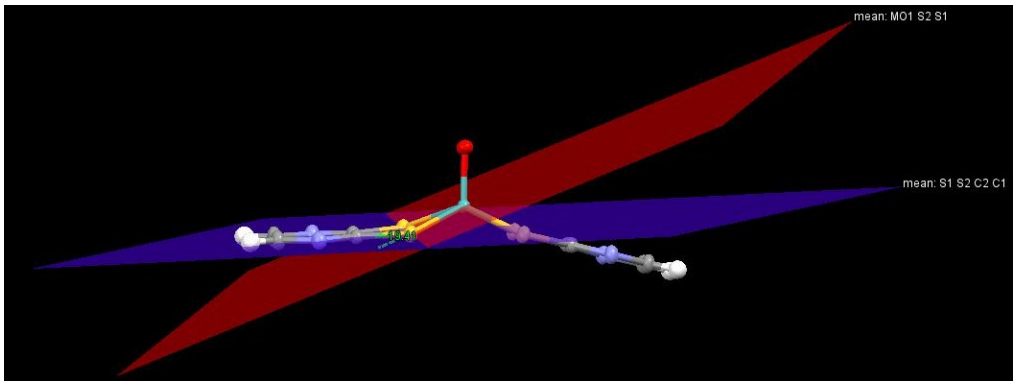

Figure S19. Fold angle b of compound $(Et_4N])_2$[IIa].

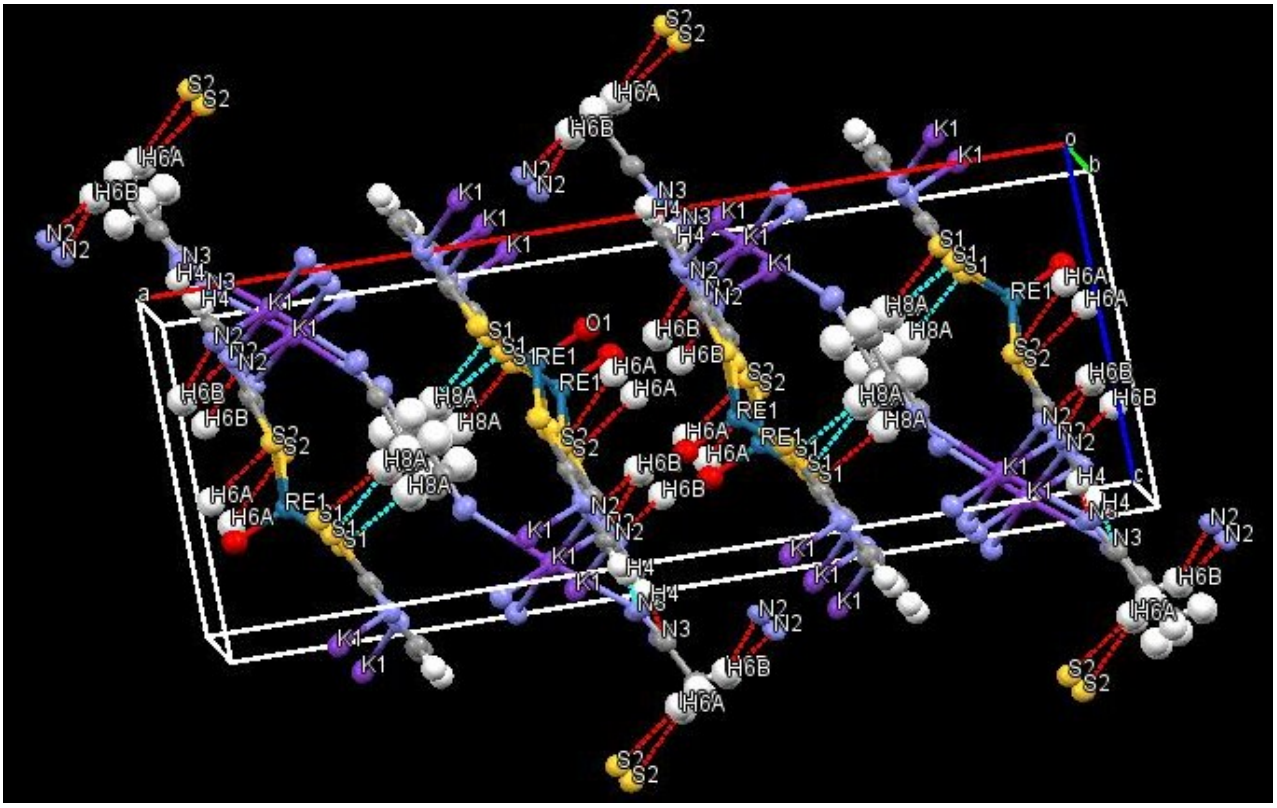

Figure S20. Unit-cell packing of compound K[IIb] with hydrogen bonds shown as dashed lines.

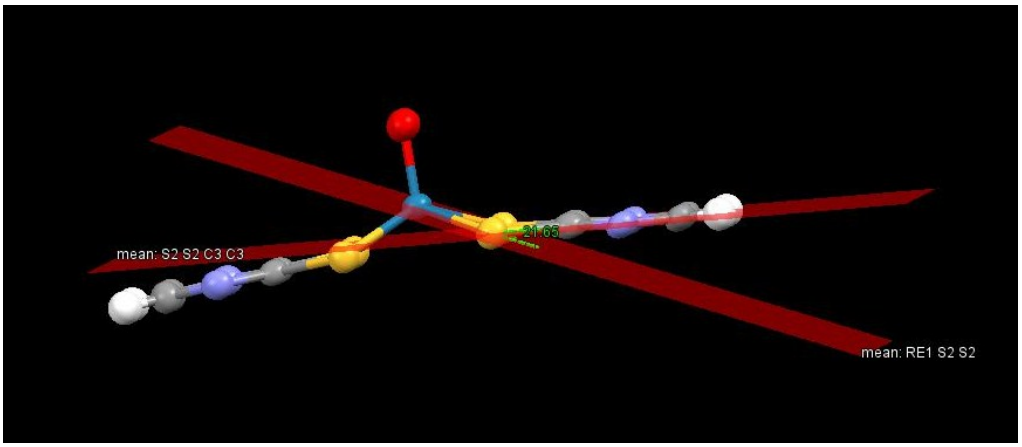

Figure S21. Fold angle of compound K[IIb].

Table S3: Mo=O distances in crystal structures of $[MoO(dithiolene)_2]^{2-}$ complexes with electron withdrawing ligand backbones (e.g. aromatic, CN^-).

Dithiolene	Mo=O distance [Å]	Reference
mnt 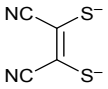	1.670	S. K. Das, P. K. Chaudhury, D. Biswas and S. Sarkar, *J. Am. Chem. Soc.* , 1994, **116**, 9061-9070.
prdt 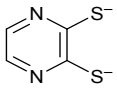	1.688	this work
dmit 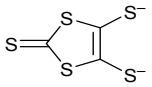	1.689	M. Atzori, E. Morra, L. Tesi, A. Albino, M. Chiesa, L. Sorace and R. Sessoli, *J. Am. Chem. Soc.* , 2016, **138**, 11234-11244.
bdt 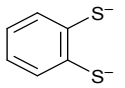	1.699	S. Boyde, S. R. Ellis, C. D. Garner and W. Clegg, *J. Chem. Soc., Chem. Commun.* , 1986, 1541-1543.
sdt 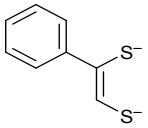	1.700	E. S. Davies, R. L. Beddoes, D. Collison, A. Dinsmore, A. Docrat, J. A. Joule, C. R. Wilson and C. D. Garner, *J. Chem. Soc., Dalton Trans.* , 1997, 3985-3995.
ndt 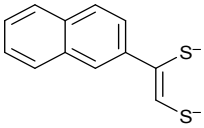	1.7023	A. C. Ghosh, P. P. Samuel and C. Schulzke, *Dalton Trans.* , 2017, **46**, 7523-7533.

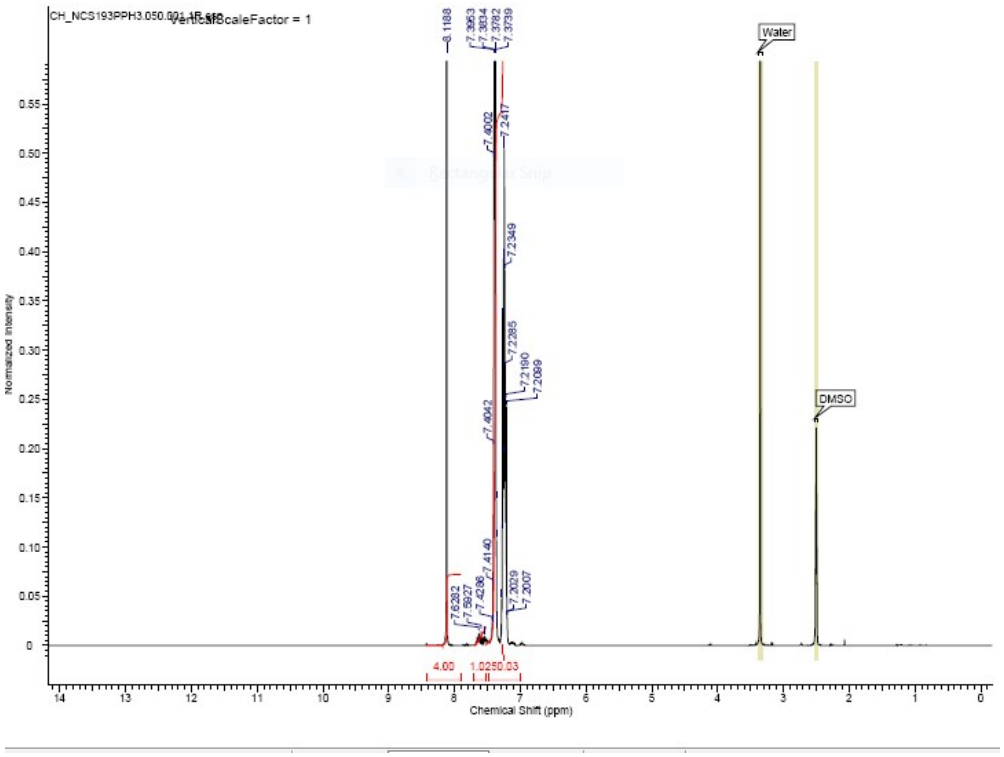

Figure S22. The 300 MHz ^{1}H NMR spectrum of compound K[IIb] with 2.5 eq. of PPh_3 in DMSO-D6 after 90 h of catalysis.

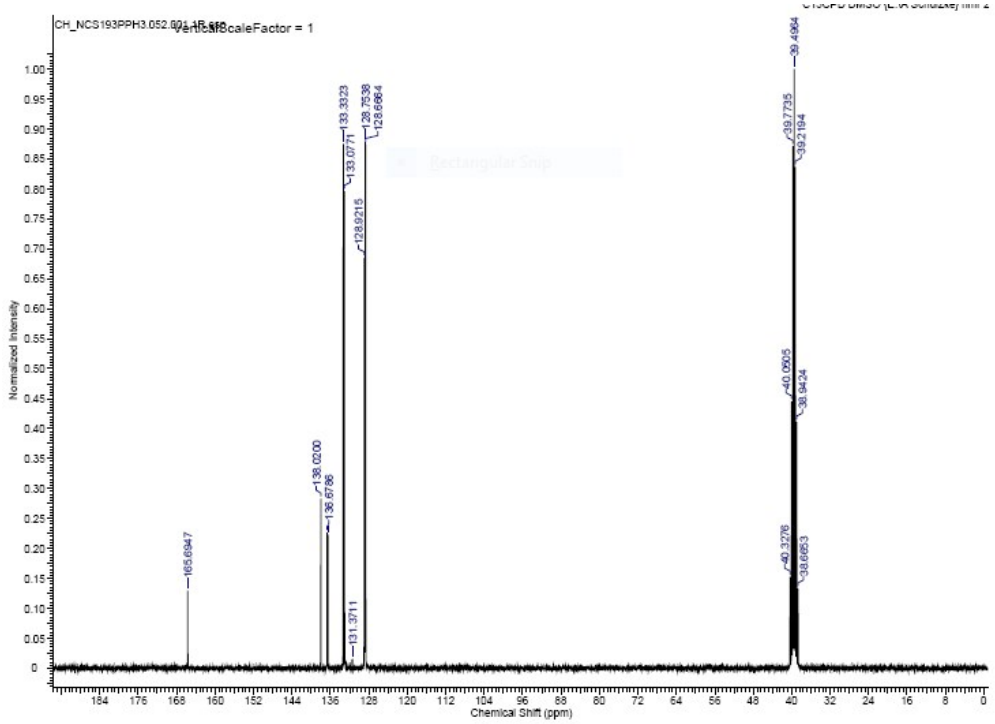

Figure S23. The 75.5 MHz ^{13}C NMR spectrum of compound K[IIb] with 2.5 eq. of PPh_3 in DMSO-D6 after 90 h of catalysis.

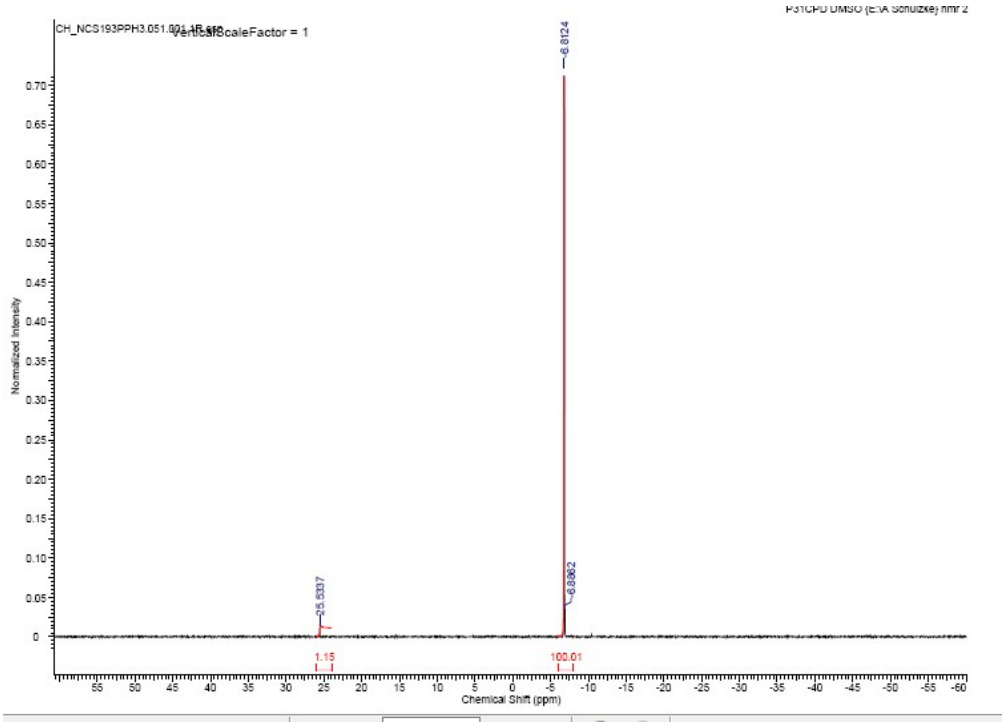

Figure S24. The ^{31}P NMR spectrum of compound K[IIb] with 2.5 eq. of PPh_3 in DMSO-D6 after 90 h of catalysis

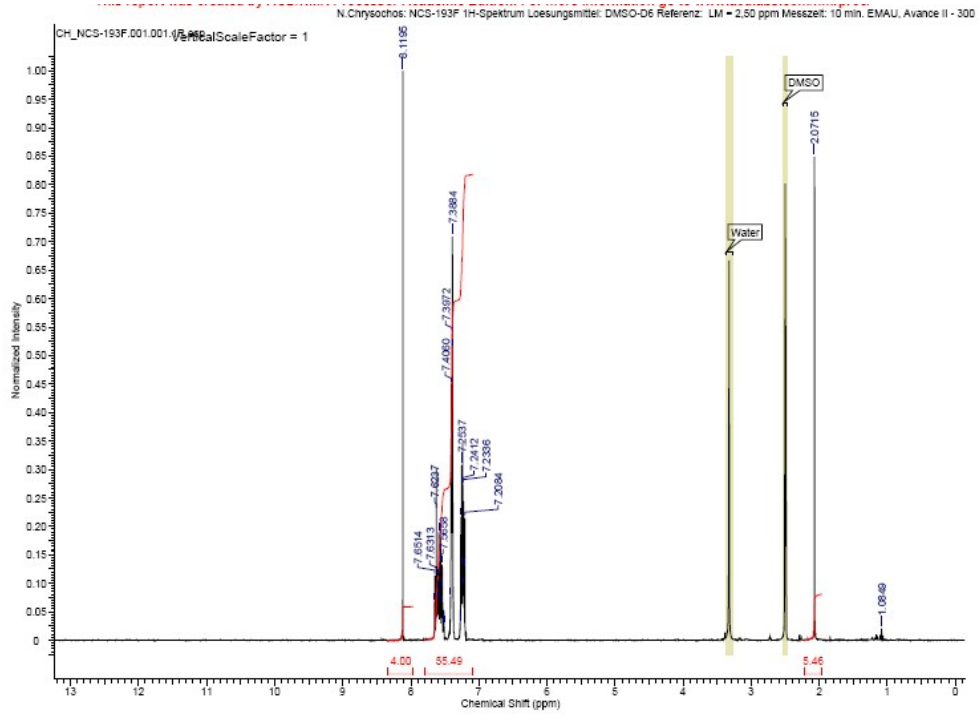

Figure S25. The 300 MHz ^{1}H NMR spectrum of compound K[IIb] with 2.5 eq. of PPh_3 in DMSO-D6 after 73 d or termination of catalytic experiment.

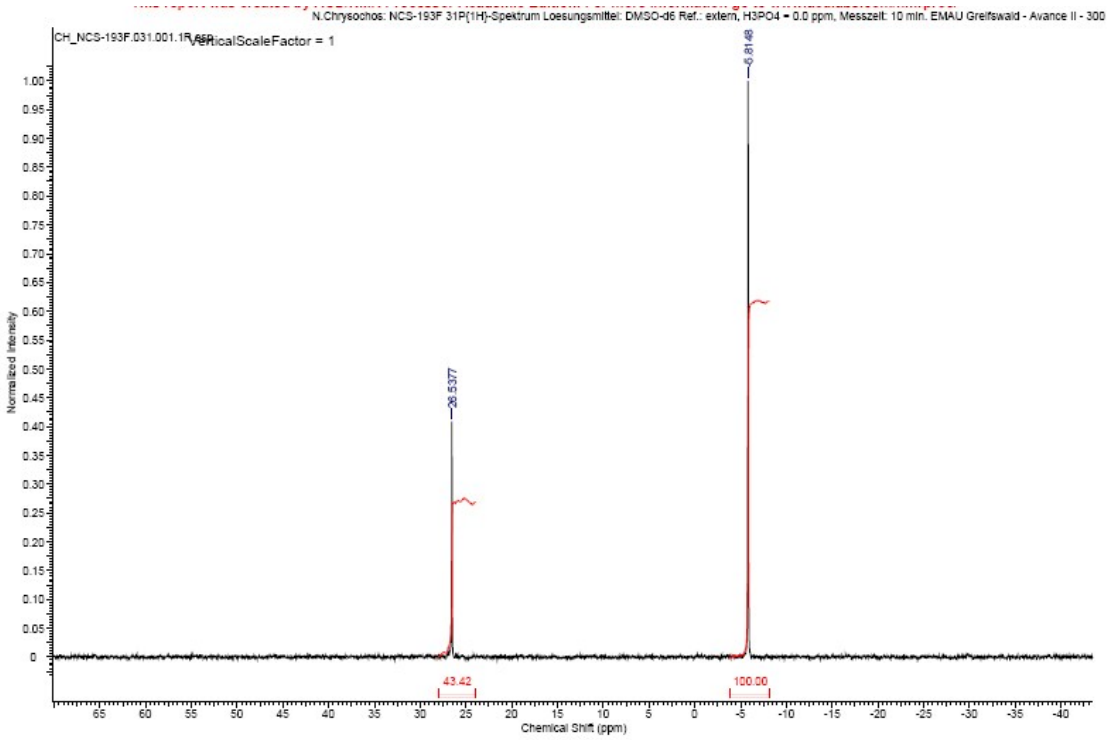

Figure S26. The ^{31}P NMR spectrum of compound K[IIb] with 2.5 eq. of PPh_3 in DMSO-D6 after 73 d (i.e. at termination) of catalytic experiment.